



## UvA-DARE (Digital Academic Repository)

### A Study of Track Reconstruction and Massive Dielectron Production in Hera-B

Hulsbergen, W.D.

**Publication date**  
2002

[Link to publication](#)

#### **Citation for published version (APA):**

Hulsbergen, W. D. (2002). *A Study of Track Reconstruction and Massive Dielectron Production in Hera-B*. [Thesis, externally prepared, Universiteit van Amsterdam].

#### **General rights**

It is not permitted to download or to forward/distribute the text or part of it without the consent of the author(s) and/or copyright holder(s), other than for strictly personal, individual use, unless the work is under an open content license (like Creative Commons).

#### **Disclaimer/Complaints regulations**

If you believe that digital publication of certain material infringes any of your rights or (privacy) interests, please let the Library know, stating your reasons. In case of a legitimate complaint, the Library will make the material inaccessible and/or remove it from the website. Please Ask the Library: <https://uba.uva.nl/en/contact>, or a letter to: Library of the University of Amsterdam, Secretariat, Singel 425, 1012 WP Amsterdam, The Netherlands. You will be contacted as soon as possible.

# Chapter 2

## The Hera- $B$ Experiment

Hera- $B$  is a fixed target experiment using the 920 GeV/c proton beam of the HERA collider at DESY in Hamburg. The experiment was proposed in 1994 with as a primary goal the measurement of  $CP$  violation in the  $B$  system, especially in the gold plated decay  $B^0 \rightarrow J/\psi K_s^0$ . Meanwhile, the Hera- $B$  detector is essentially completed. We report on the status of the detector, first physics results and the physics program for the next years.

REPRINTED (WITH PERMISSION) FROM [78]. Copyright 2001 *Acta Physica Polonica B*.

### 2.1 Introduction

The occurrence of  $CP$  symmetry violation in nature has first been observed in the decay of neutral kaons in 1964 [79]. In the standard model with 3 families  $CP$  violation arises from a non-trivial complex phase in the quark mixing matrix (*the CKM matrix*) of the weak sector of the Lagrangian [12]. Although the observations in the kaon system, together with other measurements, put constraints on the values of the parameters of the CKM matrix, they cannot yet give a conclusive test of the standard model.

A multitude of  $CP$  violating effects is expected in the decay of  $B$  mesons, some of which are cleanly predicted by the standard model. If sufficient complementary measurements are performed, it will be possible to test the standard model picture of  $CP$  violation. If the relationship between the various measurements cannot be described by a single choice of the CKM parameters, the standard model with 3 families is not a complete description of  $CP$  violation in weak decays.

A  $CP$  observable that is of specific interest is the asymmetry in the transition probability of  $B^0$  and  $\bar{B}^0$  mesons into the  $CP$  eigenstate  $J/\psi K_s$ . Uncertainties in the contribution of the strong interaction cancel in the standard model calculation of this asymmetry. Consequently, the measurement allows for a clean extraction of one of the CKM parameters, usually referred to as  $\sin(2\beta)$ .

In the last years several experiments were built to investigate  $CP$  violation in the decay of  $B$  mesons. Two new machines at KEK and SLAC produce  $B$  mesons by colliding  $e^+$  and  $e^-$  at the  $\Upsilon(4s)$  resonance. Their associated detectors BELLE and BABAR reported first results in summer 2000. Those results include preliminary measurements of  $CP$  violation in the

$B^0 \rightarrow J/\psi K_s^0$  decay mode [80, 81].

The advantage of  $b$  physics at the  $\Upsilon(4s)$  resonance is that about one out of every four interactions yields a  $b\bar{b}$  event. Furthermore, those events contain no particles besides the  $B$  meson decay products. The main limitation of the experiments are the luminosity requirements and the fact that exclusively  $B_d$  and  $B_u$  are produced. The study of  $B_s$  meson decays, which gives access to other parameters of the CKM matrix, can only be performed by experiments at hadron colliders.

Those experiments face challenges very different from the ones at the  $e^+e^-$  colliders. In hadron-hadron collisions the  $b\bar{b}$  cross section is small with respect to the total inelastic cross section. Furthermore, the  $B$  decays are superimposed on many other fragmentation products. The relative  $b\bar{b}$  cross section at the Tevatron 2 TeV/ $c$   $p\bar{p}$  collider is about  $10^{-3}$ . At the fixed target setup of the Hera-*B* experiment it is even  $10^{-6}$ .

By exploiting a wire target positioned in the halo of a 920 GeV/ $c$  proton beam, Hera-*B* is not constrained by luminosity [82]. Instead, the experiment is limited by the capacity to extract sufficient  $b\bar{b}$  events from the large inelastic background. In order to measure  $\sin(2\beta)$  with an accuracy of 0.16 in one year, the Hera-*B* experiment has to record about 1500  $B^0 \rightarrow J/\psi K_s^0$  decays. Taking into account the branching ratio of this channel of about  $9 \cdot 10^{-4}$  and the estimated trigger and reconstruction efficiency of 0.07, a total of  $4 \cdot 10^{14}$  inelastic interactions per year must be delivered. Given the collision frequency of the beam of 10 MHz and a year of  $10^7$  seconds, the experiment has to operate with a rate of 4 overlapping interactions per event.

The harsh environment of the hadron collider poses serious challenges on the design and operation of the detector. The experiment is entering a new regime of particle flux, radiation load and event rate, equivalent to LHC experiments. The main components of the detector, trigger and read out electronics were designed at the forefront of technology. As a consequence, the R&D phase took considerably longer than expected and the detector was finally completed in spring 2000, a two year delay with respect to the original schedule. The data taking in 2000 was mainly dedicated to the commissioning of the experiment. In September 2000 a machine shut down of more than a year was started in order to increase the luminosity for the  $e$ - $p$  experiments. Hera-*B* will use this period for a variety of repair and overhaul work.

The present detector performance as well as the perspectives for the next data taking are extensively discussed by the Hera-*B* collaboration in [83]. In the following sections we summarize their findings. In sections 2.2 and 2.3 we review the Hera-*B* detector and trigger components. In section 2.4 we present the physics results obtained until now. We conclude with the physics prospects for the experiment in the coming years in section 2.5.

## 2.2 The Hera-*B* detector

The Hera-*B* experiment is a forward spectrometer with a vertex detector and an extensive particle identification system. It has an opening angle of about 220 mrad in the bending plane and 160 mrad in the vertical plane. The length of the detector is roughly 20 m. A schematic overview of the detector is shown in figure 2.1. In this section we shortly discuss the different detector components.

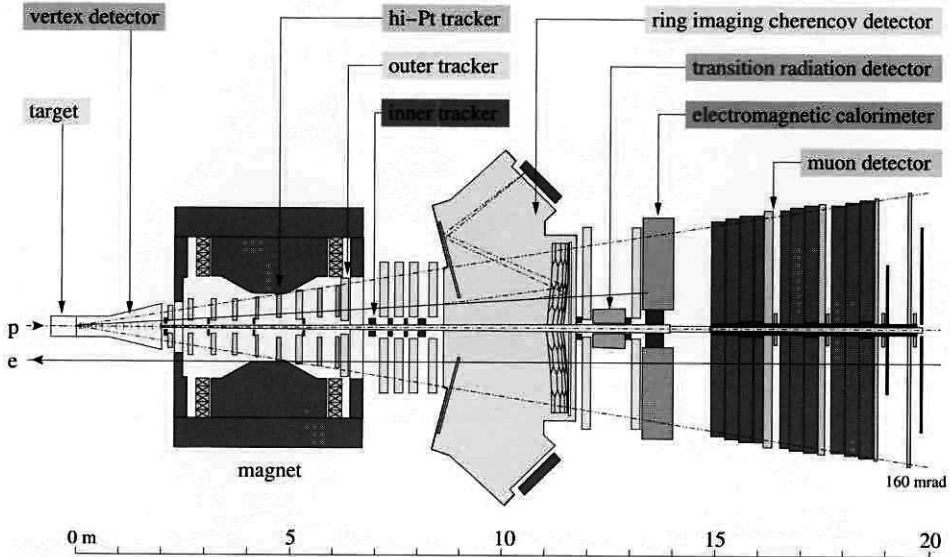


**Figure 2.1.** Schematic overview of the Hera-B detector in the  $yz$  projection. Protons come in from the left. The electron beam pipe passes through the detector at a distance of about 1 m from the proton beam pipe.

### 2.2.1 Beam and target system

The bunch crossing period of protons in the HERA accelerator is 96 ns. The energy of the beam is 920 GeV, which corresponds to a proton-nucleon cms energy  $\sqrt{s} = 41.5$  GeV and a boost  $\gamma\beta = 22.1$ . The typical decay length of  $B$  mesons is about 1 cm.

As explained in the introduction, the Hera-B experiment has to operate at an average of four overlapping interactions per bunch crossing. On the other hand accurate measurement of the decay length of the  $B$  mesons is necessary for  $B$  meson identification and time resolved asymmetry measurements. Consequently the experiment can only be performed if the primary vertices of overlapping interactions can be resolved.

A solution is found in the use of a set of 8 thin wire targets. The wire targets are moved into the halo of the beam, such that protons can be extracted without interfering with the data-taking of other detectors in the same collider. Four wires at relative angles of  $90^\circ$  are combined in one station. Two such stations are positioned along the beam at a relative  $z$  position of 4 cm. The wires can be steered individually in order to adjust the interaction rate and distribute it equally. Primary vertices can easily be separated by the vertex detector, provided that the interactions occur on different wires. The diameter of the elliptic wires is  $50 \mu\text{m}$  perpendicular to the beam and  $500 \mu\text{m}$  in  $z$ , which provides a useful constraint on the position of the primary vertices.

Currently, the target system includes wires of carbon, aluminium, titanium and tungsten, yielding an atomic mass range from 12 to 184. The simultaneous use of different target materials gives Hera-B the opportunity to perform measurements of the  $A$  dependence of various cross sections with small systematic uncertainties.

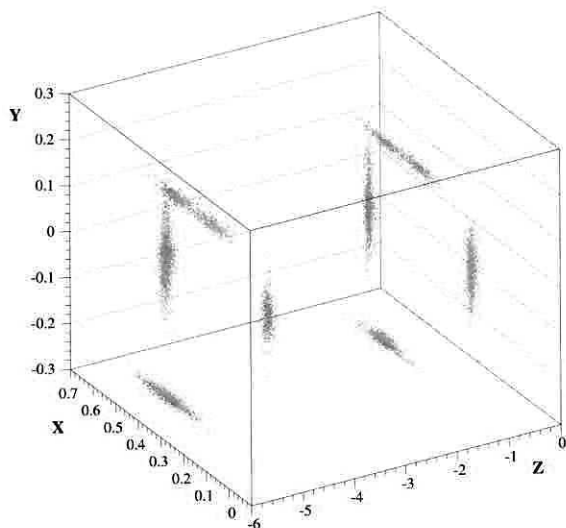


**Figure 2.2.** *xyz*-Distribution of reconstructed primary vertices when all 8 target wires are used simultaneously. The proton beam runs parallel to the *z*-axis. The units are cm.

The target system has been operated for several years and behaves according to its design specifications. Cohabitation problems at high rates with the  $e$ - $p$  experiments at HERA have been successfully solved.

### 2.2.2 Vertex detector

The vertex detector system (VDS) is a silicon strip detector with a pitch of  $50\ \mu\text{m}$ . There are 64 single and double sided  $50 \times 70\ \text{mm}^2$  modules divided over 8 stations and arranged in 4 different stereo views. The first 7 stations are mounted on a Roman pot system inside the vacuum vessel. Those can be moved away from the beam during injection and beam steering operations.

The vertex detector performs close to its design specifications. The hit efficiency is above 97% for 97 out of 116 detector planes. The stand-alone tracking efficiency is better than 95% for tracks with momentum larger than  $1\ \text{GeV}/c$ . The vertex resolution for two-track  $J/\psi$  vertices is  $60\ \mu\text{m}$  in the plane perpendicular to the beam and about  $500\ \mu\text{m}$  in the beam direction, in good agreement with Monte Carlo predictions. Figure 2.2 shows the spatial distribution of reconstructed primary vertices. One can clearly see the images of the 8 target wires.

### 2.2.3 Spectrometer

The Hera-B spectrometer consists of a dipole magnet with an integrated field of 2 Tm and a tracking system which extends over 10 m from the vertex detector up to the calorimeter. The tracker is composed of 13 superlayers, 4 of which are used in the First Level Trigger (section 2.3).

The acceptance is 220 mrad in the bending plane and 160 mrad in the vertical plane. To match the strong increase in particle flux with decreasing distance to the beam, the system is divided into two subsystems, called the *inner* and *outer* tracker respectively.

The **inner tracker** (ITR) covers distances from 5 to 28 cm from the beam axis, corresponding roughly to the forward hemisphere in the cms of the proton-nucleon collision. It has to deal with a particle flux of up to  $2.5 \cdot 10^4 \text{ mm}^{-2}\text{s}^{-1}$  and a total radiation dose of 1 Mrad per year. It is built from micro strip gas counters (MSGC) with gas electron multipliers (GEM) as pre-amplification elements.

The detector has been completed in spring 2000 after many years of intense R&D. Commissioning has not yet been finished and the overall performance needs improvement. The spatial resolution of  $80 \mu\text{m}$  is in good agreement with the design value. The hit efficiency of about 90 % is still on the low side. The inner tracker was not yet used in the trigger due to problems in the trigger output of the front-end electronics. The electronics will be replaced in the current shut down.

The **outer tracker** covers the area from the inner tracker up to the outer acceptance of the spectrometer. The detector is built from honeycomb drift chambers with wire pitches of 5 mm for the region closer to the beam pipe and 10 mm for the outer region. The largest superlayers are up to  $6.5 \times 4.6 \text{ m}^2$  in size.

Unexpectedly large sensitivity to radiation damage by highly ionizing particles caused prototypes to die within a few hours of operation. A lasting solution was only found after a long R&D program and the final production, assembly and installation of the detector was performed within one year. Since then the outer tracker has run continuously. Electronic noise related to the interface to the trigger hardware requires discriminator threshold settings substantially higher than foreseen. Consequently, the hit efficiency of 90 % and the hit resolution of  $350 \mu\text{m}$  are still poor compared to the design values of 98 % and  $200 \mu\text{m}$  respectively. Improvements by means of a revised output of the front-end drivers are being investigated.

In addition to tracking detectors, the spectrometer contains a system dedicated exclusively to the triggering of hadrons with a high transverse momentum. This system is called the **hi-Pt tracker** and it is positioned in the magnet. It consists of gas-pixel chambers for the region close to the beam pipe and straw-tube chambers with cathode pad readout for the outer region. All inner chambers were installed and operated during the 2000 run. However, the system was not yet equipped with an interface to the trigger. It will be completed in the current shut down.

### 2.2.4 Particle identification

The particle identification devices of the Hera-B detector are located downstream of the magnet. The **ring imaging Čerenkov detector** provides particle identification of pions, kaons, protons and electrons. Čerenkov light emitted by charged particles in the 2.5 m long  $\text{C}_4\text{F}_{10}$  radiator volume is projected by focal and planar mirrors in a ring image on the photo-multiplier plane. The detected rings provide information about the direction and the velocity of the particle. The relation between the observed velocity and the momentum measured in the spectrometer is used for particle identification. Figure 2.3 shows a distribution of the square of the Čerenkov angle versus the square of the inverse momentum. One can clearly see the bands corresponding to electrons, pions, kaons and protons.

The RICH system is operating at its design specifications. It provides a  $4\sigma$  separation for

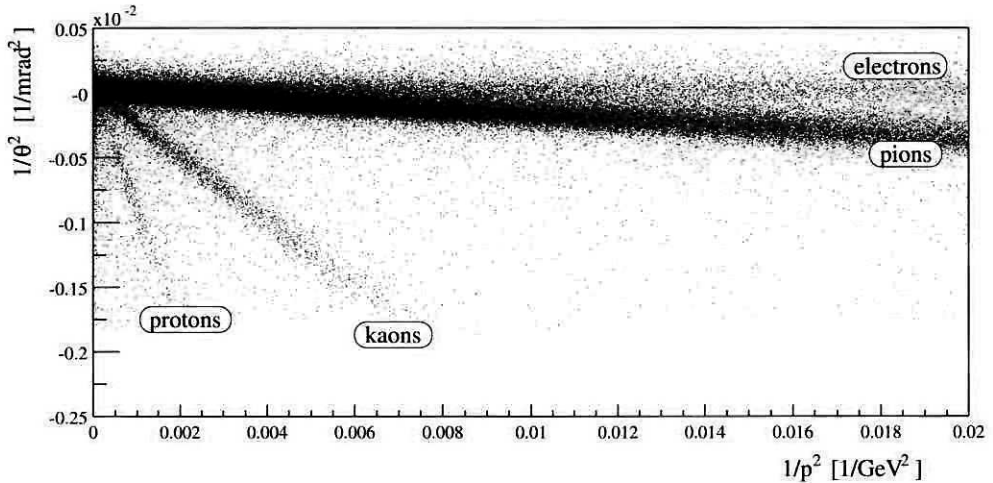


**Figure 2.3.** The square of the Čerenkov angle measured in the RICH versus the square of inverse momentum measured in the spectrometer.

electron-pion in the momentum range 3.4 – 15 GeV/c, for pion-kaon in the range 12 – 54 GeV/c and for kaon-proton in the range 23 – 85 GeV/c. (The typical momentum of a pion from a  $B$  meson decay in the Hera-B experiment is 15 GeV/c.)

The **electromagnetic calorimeter** (ECAL) provides electron and photon detection and electron-hadron separation. It produces signals for electron candidates for the trigger. The ECAL is a shashlik sampling calorimeter with Pb and W absorbers sandwiched between active layers of scintillator material. There are three lateral sections with different granularity and a total of 6000 photo-multipliers.

The ECAL was basically completed in 2000. The commissioning phase was burdened by problems with stability and hot channels. The read out suffers from considerable pick-up noise. The ECAL was calibrated using reconstructed  $\pi^0$  decays. The current energy resolution is  $\sigma(E)/E = (22.5 \pm 0.5)\%/\sqrt{E} + (17.5 \pm 0.3)\%$  in the region 12 – 60 GeV which is close to the design values. The spatial resolution is about 0.2 cm. Figure 2.4 shows the  $\pi^0$  and  $\eta$  signals observed in the two photon invariant mass distribution.

The **transition radiation detector** provides electron identification for tracks that are close to the beam pipe in the high occupancy region between RICH and ECAL. The detector consists of straw tubes and thin fiber detectors. During the last data taking period the TRD was not equipped with read out electronics. It will be completed in the current shutdown.

The **muon detector** (MUON) provides tracking for muons with a momentum larger than 4.5 GeV/c. It consists of four superlayers at different depths in iron loaded concrete absorbers. The sensitive area is covered by gas pixel chambers for the high occupancy region and tube chambers for the area further away from the beam-pipe. The tube chambers are equipped with both wire and pad read out. The latter is used in the muon trigger (section 2.3).

All components of the muon system were commissioned in the year 2000. Whereas the efficiency of the tube chambers turned out to be sufficiently high, the pad read out suffered from a

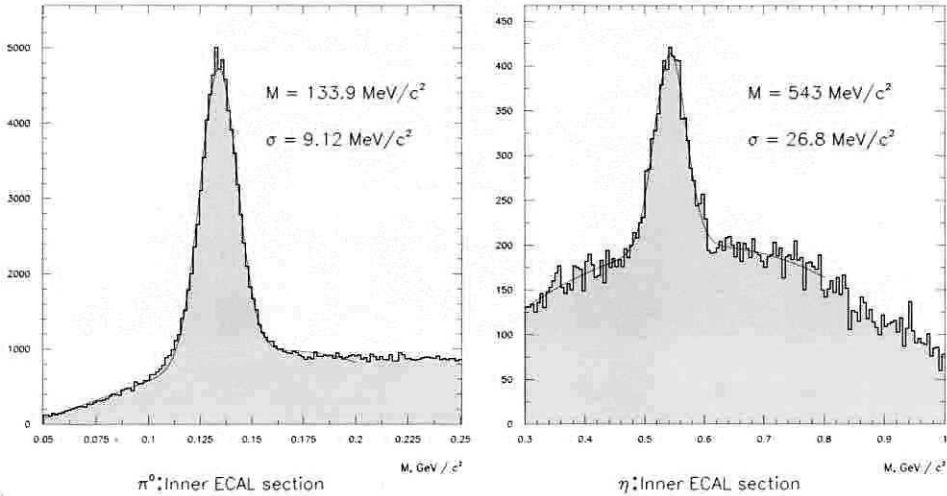


Figure 2.4.  $\pi^0$  and  $\eta$  signals observed in the two photon invariant mass distribution of the ECAL.

low hit efficiency of only 70 %, which severely reduces the muon trigger efficiency. Improvement by means of a change in the read-out electronics is under study.

## 2.3 Trigger and data acquisition system

The trigger and data acquisition (DAQ) system of Hera-B must cope with more than half a million detector channels, a 10 MHz event rate and a signal to background ratio of order  $10^{-10}$ . A solution is found in a low latency multi-level trigger with a suppression factor of about  $10^{-6}$  and a networked and high bandwidth DAQ system. Figure 2.5 shows a schematic overview of the DAQ system in connection with the different trigger levels. Input rates and latency are indicated at the right side of the graph.

The trigger is organized in four levels. The **first level trigger (FLT)** is a hardware trigger built of 60 custom-made trigger processors, interconnected and linked to the detector hardware by more than 1200 optical links. The pipe-line depth of 128 events provides a maximum latency of  $12 \mu\text{s}$ . The FLT is divided into two subsystems, called the *pre-trigger* and the *track trigger* respectively.

The pre-trigger system provides seeds or *regions of interest (RoI)* for the track trigger. There are three types of pre-trigger signals. Coincidences in the MUON pad chambers yield *muon* pre-triggers. Clusters with a high transverse energy (typically above 1 GeV) in the ECAL give electron pre-triggers. Finally, high- $p_{\perp}$  hadrons are triggered by the hi-Pt tracker. In the default  $J/\psi$  configuration the pre-trigger system gives no reduction in the event rate, since there are typically 10 pre-triggers per event. However, certain classes of pre-trigger signals can be accepted by the FLT without passing the track trigger. For example it is possible to run a high- $E_{\perp}$  photon trigger in parallel to the  $J/\psi$  trigger.

The track trigger propagates the pre-trigger seeds through the spectrometer by requiring a



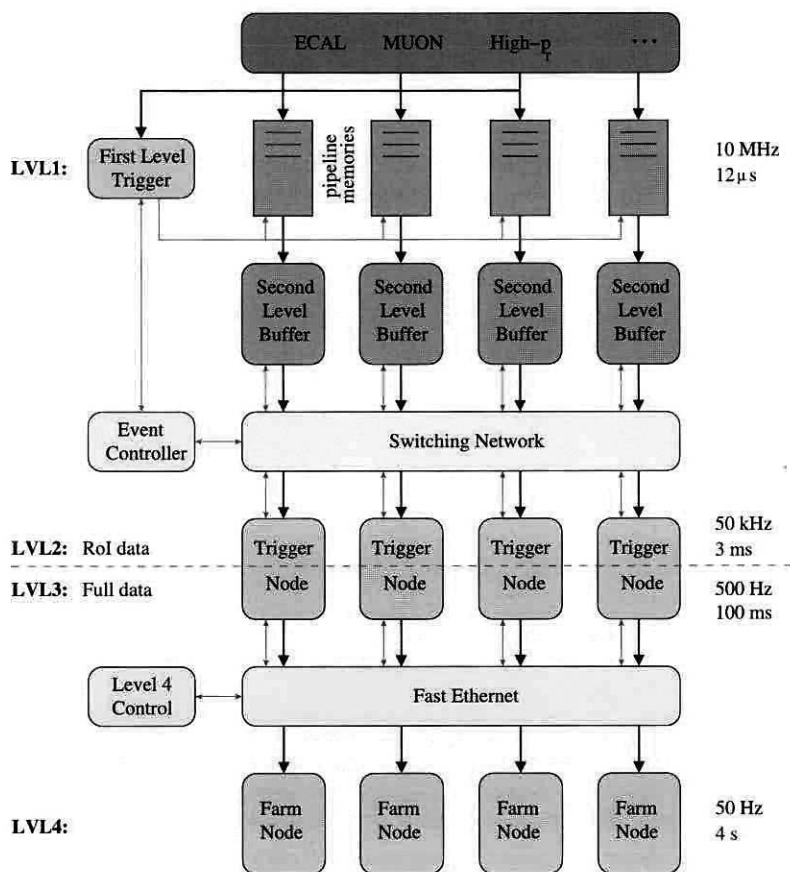


**Figure 2.5.** Schematic overview of the daq system of Hera-B. The direction of the data flow is from top to bottom. Input rates and latency are indicated on the right.

coincidence in 12 layers for the electron and high- $p_{\perp}$  seeds and 17 layers for the muon seeds. If the track search is successful, the momentum is estimated from the deflection in the magnet and a  $p_{\perp}$  cut is applied. Accepted tracks are combined into pairs after which a selection on the invariant mass can be made. Accepted events are stored in the *second level buffers* (SLB). The design efficiency of the FLT is 0.45 for  $J/\psi \rightarrow e^+e^-$  and 0.62 for  $J/\psi \rightarrow \mu^+\mu^-$ .

The **second level trigger** (SLT) is a software trigger running on a farm of 240 PCs. The SLT refines the FLT decision using information from those parts of the event that are in RoIs indicated by the FLT. Hits from all tracking and vertex detector layers are included for a re-evaluation of the FLT tracks. A vertex fit is performed to check that the trigger tracks have a common origin.

The key element in the DAQ is the switched network between the SLBs and the SLT processors. Each of the SLT nodes must have access to each of the buffers holding the event data. The switch and the buffers themselves are built on DSP processors. Protocols were developed to regulate the traffic in the switch.

Once an SLT node accepts an event it collects all detector information belonging to the event from the SLB and 'builds' the event. Afterwards, the same node calls the **third level trigger** algorithm (TLT). The TLT looks at event properties beyond the FLT tracks. For example the primary vertex can be reconstructed which allows for a selection of detached  $J/\psi$  decays. Events accepted by the SLT and TLT algorithms are sent via an ethernet switch to a second PC farm, currently 190 CPUs large. On this so called **fourth level trigger farm** (4LT) the events are reconstructed, classified and logged. The final rate at which events are stored on tape is about 50 Hz.

All the basic elements of the Hera-B DAQ and trigger system have been implemented. Although the DAQ system behaves as expected, the trigger efficiency for  $J/\psi$  events is still two orders of magnitude below the design specifications. This is both due to a low pre-trigger and a low track trigger efficiency. The electron pre-trigger is still hampered by noise in the calorimeter. The muon pre-trigger suffers from the low efficiency of the MUON pad chambers. The hi-Pt pre-trigger is not yet installed.

The most complicated system in the Hera-B trigger chain is the first level track trigger. Due to technical problems such as malfunctioning optical links the FLT could only be tested in its full extend in the last weeks of data taking in 2000, which was not sufficient for commissioning. Analysis of the correlations between FLT tracks and tracks reconstructed off-line shows that the system is technically working. Unfortunately, the concept of the track trigger is very sensitive to imperfections of both the detectors and the data transmission network. The limited hit efficiency of the tracking detectors, unresolved problems with alignment and geometry mapping as well as the technical problems mentioned above did not allow one to operate the FLT with significant efficiency.

The switching network and second level trigger farm were subjected to an extensive commissioning and debugging phase and are now operating at design specifications. The implementation of the SLT algorithm still needs fine tuning and will depend on the final performance of the FLT. A third level trigger algorithm is not yet implemented, but the possibility to select detached vertices is being investigated. The fourth level trigger farm was completed. The bandwidth for logging exceeds the design specification of 5 Mbit/s, but the time consumed by the reconstruction programs is still too large to perform all reconstruction online. During shutdown periods the system is used to reprocess the data.

## 2.4 First physics results

The period available for data taking in 2000 lasted from April when the detector was essentially completed until the end of August when the accelerator shutdown started. This period was mainly used for detector and trigger commissioning but in parallel several physics runs took place. In order to maximize the number of events with a single interaction, the target rate was kept low, typically 5 MHz. (This is an order of magnitude below the design interaction rate.) About  $2 \cdot 10^7$  events were recorded under various trigger conditions.

As described in the previous section the first level trigger was not available for data taking except at the very end of the run. Therefore, triggers were mostly provided using calorimeter and muon pre-triggers in combination with the second level trigger. The pre-triggers delivered the lepton candidates after which the SLT searched for confirmation in tracker and vertex detector

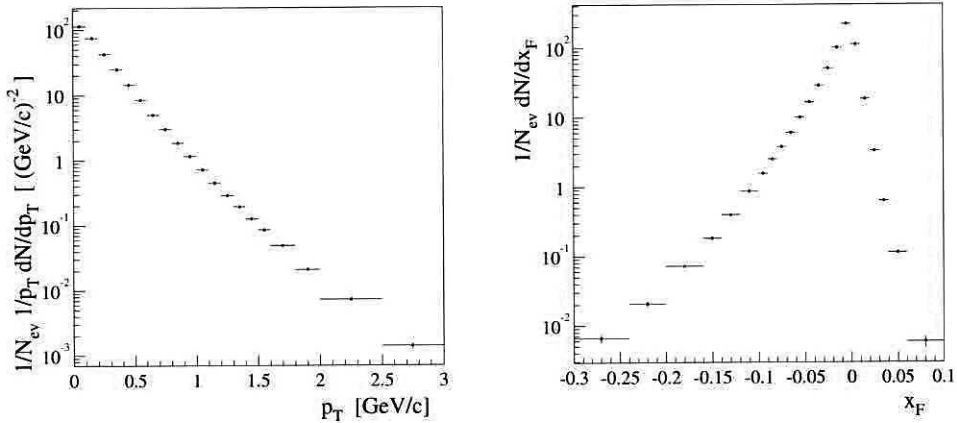


**Figure 2.6.** Inclusive particle distributions from the analysis of minimum bias data with a carbon target: transverse momentum (left) and Feynman- $x$  (right). The distributions have been normalized with the number of non-empty events — not with the number of interactions. No corrections for detector acceptance, reconstruction efficiency and ghost rate have been applied. For the calculation of  $x_F$  particles are assigned the pion mass.

and made further cuts on the  $p_{\perp}$  of the leptons and the invariant mass of the lepton pair.

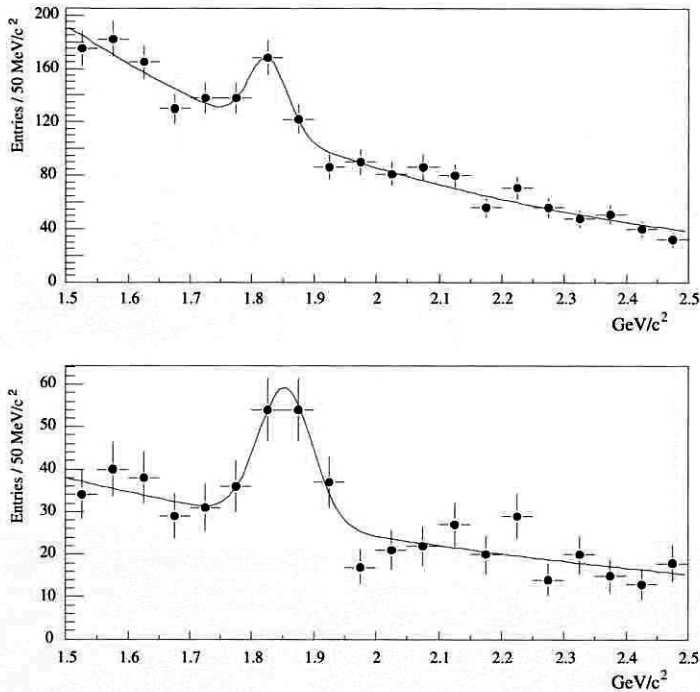
In a dedicated **minimum bias** run a sample of  $2 \cdot 10^6$  randomly triggered events was collected for target materials C, Al, Ti and W. The statistics is sufficient to compete with CERN ISR results on inclusive particle distributions [84]. Thanks to its particle identification capabilities Hera-B can extend the ISR results with measurement of the charged particle fractions. Furthermore, charged particle correlations are being studied.

Figure 2.6 shows the  $x_F$  and  $p_{\perp}$  distribution of reconstructed charged particles from the carbon run. The asymmetry of the  $x_F$  distribution is due to the missing inner tracker. The main interest of the minimum bias data for the Hera-B experiment are tuning of the luminosity determination and of the Monte Carlo event generator.

In a short **high- $E_{\perp}$  photon** triggered run a sample of about  $5 \cdot 10^5$  events with at least one ECAL cluster with  $E_{\perp} > 4$  GeV was collected. Direct photon production in hadron collisions is an interesting process in perturbative QCD due to the presence and dominance of the leading order hard quark-gluon scattering process  $qg \rightarrow q\gamma$ . Sensitivity to the initial state provides an opportunity to probe the gluon structure function in the nucleon. The amount of collected events is not yet sufficient to compete with existing measurements [85], but the observed event rate and  $E_{\perp}$  distribution agree well with the expectations.

About  $5 \cdot 10^6$  **single lepton** events were collected both with a pre-trigger SLT combination and with the full FLT track trigger. The  $p_{\perp}$  threshold for the lepton was 1.0 GeV/c for the first half of the data and 1.5 GeV/c for the other half. Reconstructed decays  $D^0 \rightarrow \pi^+ K^-$  and  $D^+ \rightarrow \pi^+ \pi^+ K^-$  show an enriched charm content of these events (figure 2.7).

The bulk of the triggered data was taken with a **di-lepton** trigger in the simplified pre-trigger-SLT configuration described at the beginning of this section. Most of this data was obtained



**Figure 2.7.** Signals of open charm decays from the single lepton triggered data:  $D^0 \rightarrow \pi^+ K^-$  (top) and  $D^+ \rightarrow \pi^+ \pi^+ K^-$  (bottom). The RICH was used for the pion and kaon identification.

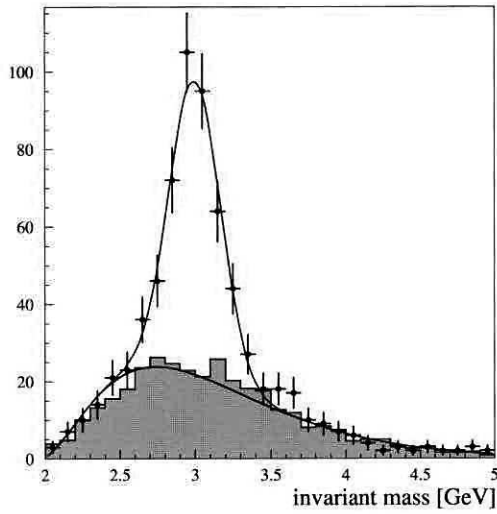
using the electron pre-trigger. Only in last two months of the run the muon pre-trigger became operational and was used in parallel to the electron trigger.

Figure 2.8 shows an  $e^+e^-$  invariant mass distribution from the analysis of part of the data sample. The shaded histogram is obtained by mixing  $e^+$  and  $e^-$  candidates from different events. In order to enrich the fraction of real leptons an associated Bremsstrahlung cluster was required in the off-line analysis. The efficiency of this identification ‘trick’ is about 30% per lepton. The width of the  $J/\psi$  signal is  $\sigma_{ee} \sim 120 \text{ MeV}/c^2$ , which is roughly a factor of 2 larger than for the  $J/\psi \rightarrow \mu^+\mu^-$  signal. The difference can be explained by a worse lepton momentum determination due to unrecovered Bremsstrahlung loss.

Figure 2.9 shows the  $\mu^+\mu^-$  invariant mass distribution. Signals of both  $J/\psi$  and  $\psi(2s)$  are evident. The total sample contains about 4000  $J/\psi$  events. The  $J/\psi$  mass resolution of  $\sigma_{\mu\mu} \sim 55 \text{ MeV}/c^2$  is about 30% worse than in Monte Carlo. The difference can be attributed to a still preliminary alignment.

The  $J/\psi \rightarrow \mu^+\mu^-$  events are combined with calorimeter clusters for the reconstruction of  $\chi_c \rightarrow J/\psi\gamma$  decays. Figure 2.10 shows the difference between the reconstructed  $J/\psi\gamma$  invariant mass and the reconstructed  $J/\psi$  mass. The filled histogram is obtained by event mixing. A clear enhancement in the expected mass region is observed. The statistics is not yet sufficient to distinguish the  $\chi_{c,1}$  and  $\chi_{c,2}$  states.

The di-muon data sample is also used to tune the vertexing software. The final goal is to detect



**Figure 2.8.** Positron-electron invariant mass distribution. The shaded histogram is obtained by combining  $e^+$  and  $e^-$  from different events.

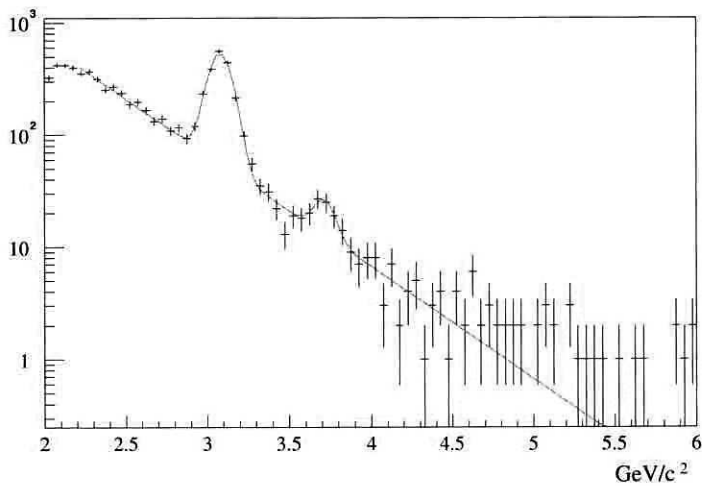


**Figure 2.9.** Di-muon invariant mass distribution with signals of the  $J/\psi$  and the  $\psi(2S)$ . The background is described by an exponential.

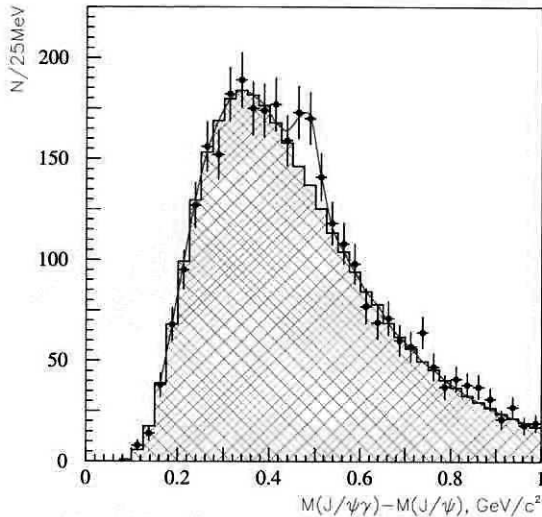


**Figure 2.10.** Invariant mass difference of  $\mu^+\mu^-\gamma$  and  $\mu^+\mu^-$  in the  $J/\psi$  mass window. The shaded histogram is the background estimated with mixed events.

detached vertices in order to determine the  $b\bar{b}$  cross section. Figure 2.11 shows the distance along the  $z$ -axis between the  $J/\psi$  vertex and the primary vertex. The peak centred at zero has a width of approximately  $630\ \mu\text{m}$ . It corresponds to muon pairs originating from the primary vertex. The  $J/\psi$  mesons emerging from  $B$  decays should have a positive  $\Delta z$ , the typical decay length being about 1 cm. Assuming a cross section of 12 nb (based on existing measurements [26, 27]) only 2 detached  $J/\psi$  events are expected. The present statistics can therefore not be conclusive. Optimization of the software tools and alignment is in progress in order to understand and reduce the tails in the vertex distribution.

It is evident that a measurement of the  $b\bar{b}$  cross section can only come from an analysis of the full  $J/\psi$  sample collected with the electron trigger. We estimate that this sample contains about  $3 \cdot 10^4$   $J/\psi \rightarrow e^+e^-$  events including about 20  $B \rightarrow J/\psi X$  decays.

## 2.5 Physics prospects

In 2001/2002 the Hera- $B$  collaboration will concentrate on making measurements which contribute to the understanding of QCD, such as charmonium and heavy flavour production. Possibly charm physics topics can be addressed as well, although this will require a revised trigger scheme. The physics program is shaped by the status of the detector and trigger at the end of the 2000 run and a conservative extrapolation based on repairs and upgrades that are currently being addressed. The physics goals in order of the level of confidence that they can be reached are:

- Measurement of the  $b\bar{b}$  cross section. The two existing measurements at fixed target energies are incompatible and have poor precision [26, 27]. Measurement of the cross section is important for further constraints on NLO QCD predictions.

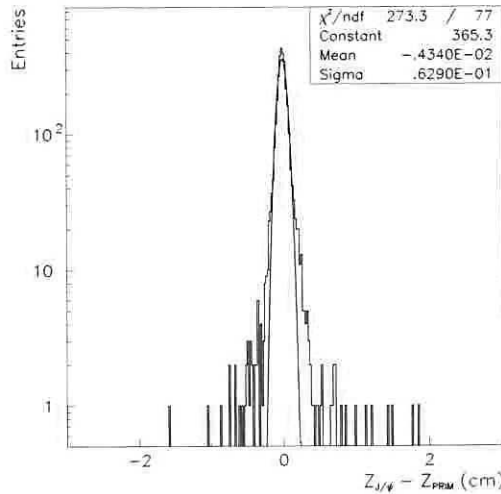


**Figure 2.11.** Distance in  $z$  between the reconstructed primary vertex and the  $J/\psi \rightarrow \mu^+ \mu^-$  vertex. The line represents a fit of a Gaussian to the core of the distribution.

- Measurement of  $J/\psi$ ,  $\psi'$  and  $\chi_c$  production cross section, decay angular distribution and  $A$  dependence. Quarkonium production is a rich field for the experimental study of QCD. The mechanisms for quarkonium production are still poorly understood. More measurements are required to distinguish between different production models, such as the colour singlet and colour octet model [69]. In addition some information on the high- $x$  gluon structure function can be obtained.

Currently measurements are only available in the forward hemisphere. Hera-B can extend the measured range to negative  $x_F$  where predictions of charmonium suppression effects from different models are more distinct.

- Measurement of the angular distribution of Drell-Yan pairs. Results from NA10 [86] and E615 [87] in pion-nucleon scattering indicate a violation of the Lam-Tung relation and consequently do not agree with perturbative QCD predictions. Hera-B can provide a first measurement with incident protons.
- Measurement of the  $\Upsilon$  production cross section, decay angular distribution and  $A$  dependence. The physics issues are the same as for the charmonium measurements discussed above.
- Measurement of the direct photon production at high- $p_{\perp}$ . The hard photon spectrum is sensitive to the gluon structure function. Previous experiments show significant deviations from NLO QCD calculations [85].
- Improvement of the upper limit on the  $D^0 \rightarrow \mu^+ \mu^-$  branching fraction. Any measurable signal in this channel would indicate physics beyond the standard model. Hera-B can substantially improve on the currently published upper limit [88].
- Measurement of Drell-Yan production at high- $p_{\perp}$ . Although a more difficult measure-

ment, high- $p_{\perp}$  Drell-Yan production provides a cleaner probe to the high- $x$  gluon structure function than high- $p_{\perp}$  photons (see above).

- Accumulation of an open charm sample large enough to allow meaningful measurements of properties of charm decays. An example is the lifetime ratio  $D^0 \rightarrow K^- \pi^+$  to  $D^0 \rightarrow K^- K^+$ , where measurements by Focus indicate a  $2\sigma$  deviation from standard model predictions. (See [89] for an overview.) An algorithm is being developed to detect secondary vertices at the third level trigger in order to extract efficiently the high rate of charm.

In parallel to the data taking the Hera- $B$  collaboration hopes to improve detector and trigger performance up to a level close to the design specifications in order to continue with a competitive heavy flavour program after 2002. By that time  $CP$  violation in the golden decay  $B^0 \rightarrow J/\psi K_s^0$  will have been established with a precision beyond the reach of the Hera- $B$  experiment. Therefore, Hera- $B$  will mainly focus on  $B_s$  physics, rare  $B$  decays and exclusive  $B \rightarrow J/\psi X$  lifetimes.

## 2.6 Conclusions

As indicated in this report the Hera- $B$  detector is essentially completed. Many subsystems perform close to the design specifications. However, the first level trigger, the most crucial part of the experiment, could not be operated with significant efficiency in the period before the shutdown of the accelerator.

The next data taking starts early 2002. In the year 2002 the Hera- $B$  collaboration will mainly focus on the study of QCD in proton-nucleon collisions with special attention to quarkonium production, Drell-Yan production and high- $p_{\perp}$  photon physics. In parallel the detector and trigger will be improved in order to reach a performance close to the design specifications of the experiment. When such a performance is achieved the Hera- $B$  experiment can make valuable contributions to the study of  $b$  physics and  $CP$  violation, in spite of the delay in its commissioning and the corresponding head-on start of competing experiments.



